

POST-FIRE THIN DEBRIS FLOWS: SEDIMENT TRANSPORT AND NUMERICAL MODELLING

EMMANUEL J. GABET*

Department of Geological Sciences, UC Santa Barbara, Santa Barbara, CA 93106, USA

Received 22 January 2002; Revised 11 November 2002; Accepted 5 March 2003

ABSTRACT

The creation of a hydrophobic layer in the soil during fires in semi-arid environments inhibits the infiltration of rainfall. This leads to increased rates of runoff and associated sediment transport. When the hydrophobic layer is deposited beneath the soil surface, a perched water table develops which may cause thin (1–2 cm) hillslope failures that are distinguishable from features caused by rilling and sheetflow. Evidence for these failures was observed after a fire near Santa Barbara, California. The amount of sediment eroded from some hillslopes was substantial, with 290 kg of sediment per metre width of hillslope delivered to the valley floor. The mechanics of these failures are examined with a numerical model that incorporates a stability analysis with subsurface flow routing along a typical hillslope profile. The model correctly predicts the location of the failures as well as the rainfall amount necessary to trigger them. Copyright © 2003 John Wiley & Sons, Ltd.

KEY WORDS: erosion; geomorphology; fire; sage scrub; hydrophobic soils

INTRODUCTION

Fires amplify most hillslope sediment transport processes (Swanson, 1979) and transport by runoff processes is particularly intensified by the creation of a hydrophobic layer (DeBano *et al.*, 1979). Fires create hydrophobic layers when vaporized organic matter condenses on the soil surface or at some depth in the soil (DeBano *et al.*, 1979; DeBano, 1981). Depending on the depth of the hydrophobic layer, increased sediment transport from hillslopes by runoff can take two different forms. In the first, increased soil hydrophobicity at the soil surface leads to higher rates of surface runoff that transports sediment downslope (Cerdeña, 1998; Prosser and Williams, 1998; Soto and Diaz-Fierros, 1998). In the second, a hydrophobic layer deposited at some depth within the soil creates a shallow perched water table during rainstorms. If pore pressures within this saturated zone become sufficiently high, shallow slope failures are triggered which mobilize as thin debris flows (TDFs) and strip the top layer of soil (Figure 1) (Wells, 1987). Because the creation of a hydrophobic layer at depth in the soil is common after fires in Mediterranean environments (Krammes and DeBano, 1965; DeBano, 1981), erosion by TDFs is undoubtedly much more common than reported and may be incorrectly attributed to rilling and sheetflow. Additionally, TDFs are not limited to Mediterranean environments, they have been observed in a pine forest in New Mexico (Cannon *et al.*, 2001) and even in a tropical dry forest in Nicaragua (R. Dull, personal communication).

Rainfall following a fire in coastal sage scrub near Santa Barbara, California, resulted in substantial amounts of sediment transported from several hillslopes. In this contribution, I report field observations of sediment transport by TDFs and I present a numerical model for predicting the location of TDFs along a hillslope profile. This model couples a subsurface flow routing algorithm with an infinite-slope stability analysis to explore the conditions leading to these failures.

FIELD OBSERVATIONS

In the autumn of 1999, a prescribed burn was conducted on the Midland School property in the Santa Ynez Valley near Santa Barbara, California. The purpose of the fire was twofold: to reduce fuel load and to convert

* Correspondence to: E. J. Gabet, Department of Geology, University of Montana, Missoula, MT 59812, USA. E-mail: gabet@selway.umt.edu

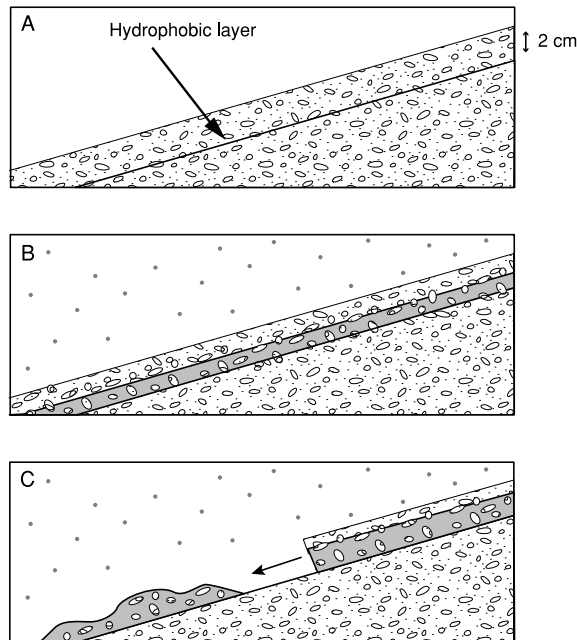


Figure 1. (A–C) Sequential events leading to the initiation of thin debris flows. During a rainstorm, the hydrophobic layer creates a perched water table that may cause a small debris flow. Modified from Wells (1987)

coastal sage vegetation to grassland for pasturage. The area is hilly with soil-mantled convex hillslopes. Soil depths range from 0.1 to 0.3 m on the planar hillslope sections and typical hillslope angles range from 25° to 30°. The regional climate is semi-arid Mediterranean and the lithology is poorly consolidated Plio-Pleistocene fanglomerates of the Paso Robles Formation (Dibblee, 1993). The hillslopes are primarily vegetated by California sagebrush (*Artemisia californica*) and purple sage (*Salvia leucophylla*). Although the air temperature during the fire was 24 °C and the relative humidity was 44 per cent, there were large patches of intense burning. According to data summarized by DeBano *et al.* (1979), these may be identified by white ash deposits that indicate temperatures over 650 °C.

Simple experiments were performed on the hillslopes before and after the fire to investigate changes in runoff processes. These consisted of quickly pouring one litre of water onto the soil surface. Before the fire, the water simply infiltrated through the soil. However, two weeks after the fire, the experiments yielded dramatically different results. While the water was being poured, a thin layer of soil 1–2 cm thick would liquefy and move downslope with a steep-faced snout composed of coarse particles (similar observations were made by Wells (1987)). As the slurry progressed, it would entrain more soil along its path and leave small levees on either side (Figure 2). After passage of the slurry, the soil that remained was dry, revealing the presence of a hydrophobic layer. The depth of the hydrophobic layer was coincident with the lower boundary of a biotic crust composed of a porous mineral soil thickly interwoven with fine roots and moss (Fierer and Gabet, 2002). DeBano (1981) and DeBano *et al.* (1979) emphasize the importance of a thermal gradient through the soil rather than the absolute temperatures in the creation of the hydrophobic layer. The sharp textural discontinuity between the biotic crust and the underlying soil likely created a steep thermal gradient that enhanced the condensation of the hydrophobic layer at this depth.

Sediment transport during the first rainstorms after the fire appears to have been by the same process described in the experiments above. This conclusion is based on the presence of small, 1–3 cm high levees that were deposited on both sides of long, linear rill-like features. Although bearing a superficial resemblance to rills formed by overland flow, the scars left by the TDFs had rectangular cross-sections and were 5–15 cm wide but only 1–2 cm deep. Similar features have also been observed by Cannon *et al.* (2001) after a fire in a pine forest in New Mexico. The head scarp of many of the scars at Midland School were located at the topographic

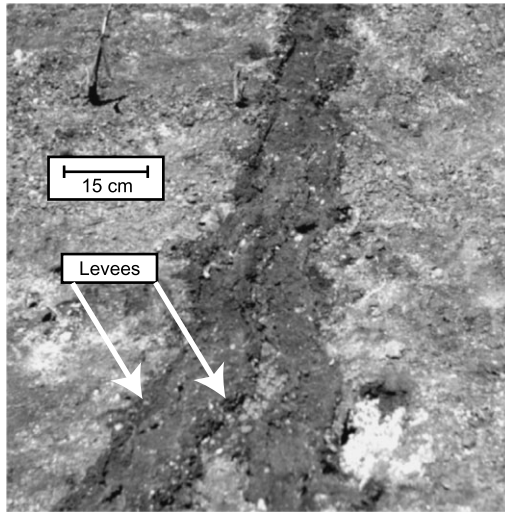


Figure 2. Levees formed by a small debris flow caused by pouring water on burnt soil after a prescribed burn

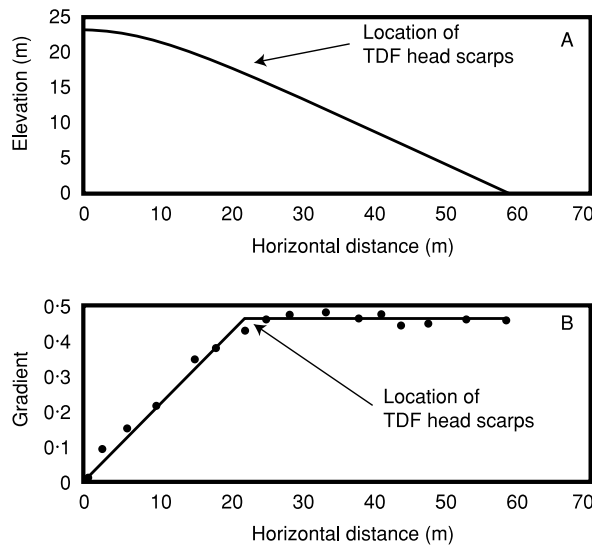


Figure 3. (A) Profile of hillslope where 60 per cent of the soil surface was stripped by TDFs. Arrow designates the location of the head scarps of many of the failures. (B) Gradients along the hillslope profile in (A). The filled circles represent the calculated gradients from the survey data. Many TDFs began at the topographic transition where the hilltop convexity leads into the straight midslope. The line represents the gradients of the smoothed profile used in the numerical model

transition where the divide convexity leads into the straight mid-slope section (Figure 3). The levees were composed entirely of mineral soil because the fire had completely consumed the litter and the ash had previously been blown away by wind. The composition of these small levees differs from those observed by Cannon and Reneau (2000) after a fire. Cannon and Reneau (2000) describe small levees composed primarily of organic material and they hypothesize that the levees were formed by overland flow pushing aside litter on the soil surface.

Further evidence that the levees studied at Midland School were formed by debris flows is shown in Figure 4. In this photograph, the levees of a TDF extend past the burnt hillslope and down across the grassy valley floor. This is significant for two reasons. First, upon reaching the valley floor, overland flow would likely

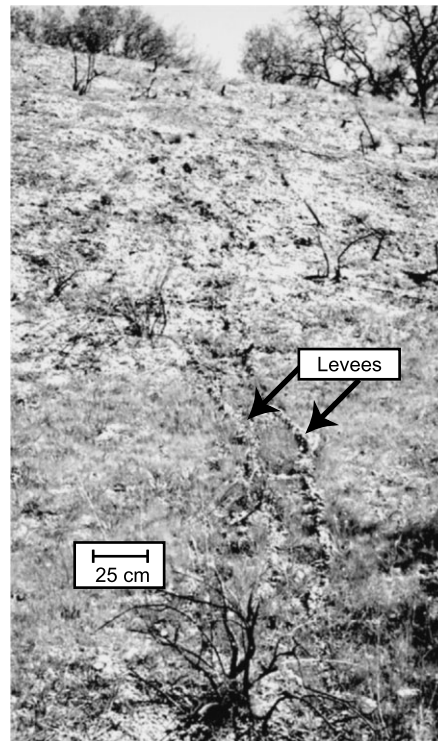


Figure 4. Debris flow levees. The TDF began on a steep burnt hillslope and travelled across the valley bottom. The distance between the levees is approximately 25 cm

have spread out rather than followed along a confined path. Second, the levees on the valley floor could not have been formed by pushing aside loose debris since the soil is tightly bound by the grass roots.

On one particular hillslope (profile shown in Figure 3), approximately 60 per cent of the hillslope surface below the topographic transition was stripped by these debris flows to a depth of 1–2 cm. Substantial amounts of sediment, both coarse- and fine-grained, were deposited on the valley floor. The mass of mineral sediment per unit width of hillslope delivered to the valley can be estimated from:

$$\frac{\text{mass}}{\text{unit width}} = Adl\rho_s(1 - P) \quad (1)$$

where A is the fraction of the area covered by TDF scars, d (m) is the average depth of the scars, l (m) is the average scar length, ρ_s is the bulk density of the top layer of soil (560 kg m^{-3} ; 1 s.d. = 10; $n = 4$), and P is the fraction of plant material, by weight, in the crust (0.037; 1 s.d. = 0.012; $n = 8$). The average scar depth and length are 1.5 cm and 60 m, respectively. The measured particle density of the mineral fraction of the biotic crust was measured to be 2320 kg m^{-3} (1 s.d. = 70; $n = 6$). From Equation 1, the calculated mass of sediment delivered by TDF to the valley from each unit width of hillslope is 290 kg (this represents a maximum value because a small portion of the sediment was left on the hillslopes as levees). If the deposited sediment has a porosity of 50 per cent and the regional fire recurrence interval is 47 years (Keeley *et al.*, 1999), the long-term deposition rate is $0.005 \text{ m}^3 \text{ a}^{-1}$ per unit length of valley. Because the sage vegetation is nearly completely consumed during fires, I was unable to find any charcoal for radiocarbon dating in the valley fill; this would have provided a means for assessing the validity of the estimated long-term deposition rate. However, Equation 1, in conjunction with a stability analysis (see later), was incorporated into a stochastic sediment delivery model (Gabet and Dunne, in press) that includes the suite of hillslope transport processes, such as dry ravel (Gabet, 2003) and shallow landslides (Gabet and Dunne, 2002). Results from the model were compared to reservoir sedimentation records

and found to accurately predict the total sediment yield from modelled watersheds. Additionally, this model estimates that TDFs account for nearly 60 per cent of the total sediment yield from steep, sage-scrub hillslopes. Finally, given the same values as above, the long-term bedrock lowering rate is approximately $8 \times 10^{-5} \text{ m a}^{-1}$.

The amount of sediment delivered to the valley is dependent on the path length of the TDFs. The location of the head scarps near the divide, however, is counter-intuitive. In the absence of cohesion, the two opposing forces on a landslide mass are the disturbing force and the resisting force, represented by the shear stress and the normal stress, respectively (Selby, 1993). Over the time-scale of a rainstorm, the shear stress remains constant but, as the pore pressure increases, the normal stress decreases. With sufficient rainfall, the normal stress may decrease enough such that it is unable to resist the shear stress and the landslide fails. On a slope, changes in the normal stress will depend only on changes in pore pressure and pore pressures should increase downslope as the lower portions of the slope receive water from upslope as well as from direct precipitation. Given this simple description of the pore pressure field, the failures should occur near the base of the slope yet most failure scarps were observed close to the divide. In the following analysis, I present a physical explanation for the location of the head scarps.

NUMERICAL MODEL

Hydrological properties of the crust

Values for certain hydrological characteristics of the biotic crust are needed for the numerical model. The porosity of the biotic crust was measured by saturating a known volume of the dry crust collected in a sampling ring. From four samples, the average porosity was 0.71 ± 0.01 (1 s.d.). The saturated hydraulic conductivity was measured with a falling-head permeameter (Fetter, 1997). From three undisturbed samples, the average saturated hydraulic conductivity was found to be $0.0005 \pm 0.0002 \text{ m s}^{-1}$ (1 s.d.).

Stability analysis

The failure mechanics of TDFs may be considered identical to shallow landslides with an impermeable boundary leading to slope-parallel subsurface flow. A force balance based on the infinite slope assumption (Selby, 1993) is often used to analyse slope stability in shallow landslides:

$$F = \frac{C + \{[m\gamma_{sc} + (1 - m)\gamma_m - m\gamma_w]z \cos^2 \theta\} \tan \phi}{[m\gamma_{sc} + (1 - m)\gamma_m]z \cos \theta \sin \theta} \quad (2)$$

where C is total cohesion from both soil and roots (kPa), F is factor of safety, m is ratio of water depth to soil depth, z is failure depth measured vertically (m), γ is unit weight (sc = saturated colluvium, m = moist colluvium, w = water) (kN m^{-3}), θ is hillslope angle ($^\circ$) and ϕ is internal angle of friction ($^\circ$).

F represents the ratio of resisting forces to disturbing forces and the slope is stable when $F > 1$. Values for z , γ , and ϕ were measured for the hillslope shown in Figure 3 (Table I). Because the soil is loose and coarse at the surface, soil cohesion is zero and any apparent cohesion from the fine roots in the biotic crust is assumed to be zero because the roots were dead and brittle after the fire. The ratio m is calculated as:

$$m = \frac{h}{z \cos \theta} \quad (3)$$

Table I. Values for stability analysis

z (m)	0.015
γ_{sc} (kPa m^{-1})	11.0
γ_m (kPa m^{-1})	8.5
γ_w (kPa m^{-1})	9.8
θ ($^\circ$)	33*

* Measured with a shear vane.

where h is the subsurface flow height measured orthogonal to the impermeable layer (Beven, 1981; Dunne, 1991).

Subsurface flow routing

The hydrologically active depth of soil is taken to be 1.5 cm, with an impermeable base to simulate the hydrophobic layer. Conservation of mass is achieved through a finite-difference solution of the one-dimensional continuity equation:

$$\frac{\partial q}{\partial x} + p \frac{\partial h}{\partial t} = i_e \quad (4)$$

where q is unit discharge, x is distance downslope, p is porosity, t is time, and i_e is effective rainfall intensity. Effective intensity is calculated along the length of the hillslope from:

$$i_e = i \cos \theta \quad (5)$$

Effective rainfall intensity is used instead of a spatially averaged intensity because, assuming vertical rainfall, the rainfall flux per unit area of slope will be higher on the gentle slopes than on the steep slopes. This results in a 10 per cent reduction in rainfall intensity from the divide to the midslope section for the hillslope in Figure 3. This is an important detail because if the downslope flow of water through the biotic crust is less than the rainfall intensity during the early moments of a rainstorm, the pore pressure response at any point on the hillslope will initially be dominated by local precipitation rather than subsurface flow accumulation.

Subsurface discharge, q , is calculated according to Darcy's law:

$$q = hK \frac{dH}{dx} \quad (6)$$

where K is saturated hydraulic conductivity, and dH/dx is the total hydraulic head gradient. On steep slopes, dH/dx may be approximated by (Beven, 1981):

$$\frac{dH}{dx} = \frac{dh}{dx} \cos \theta - \sin \theta \quad (7)$$

Note that the time for the rainwater to reach the perched water table is considered to be negligible. Ideally, unsaturated flow along this path should be determined with Richards' equation (Richards, 1931); however, the short vertical path length suggests that the time scale for infiltration is much less than for lateral flow.

The one-dimensional model is run with a 1 m mesh size and 1 s time step. The hillslope in Figure 3 provides the topographic template and was smoothed to prevent numerical instabilities. Factor-of-safety values are calculated at each node according to Equation 2 at every time step to determine whether a failure is triggered. The 2 h rainfall series used as model input comes from a local recording rain gauge (Figueroa Mountain Ranger Station) at the time that the TDFs are thought to have occurred. The rainfall intensity during this time was 2.5 mm h⁻¹.

Results

Model results leading up to and including the time of failure are presented in Figure 5. After 0.7 h, factor-of-safety values are above unity along the length of the entire hillslope and subsurface flow depths reflect the spatial variation in precipitation intensity. At 1.05 h, flow depths have increased and the 'doming' of the water table at the hillslope divide has become more pronounced. Because the saturated hydraulic conductivity is low and the hydrologically active layer is thin, the height of the water table anywhere along the hillslope is dominated by local precipitation rather than downslope flow accumulation. For this reason, factor-of-safety values drop below unity simultaneously along the entire linear portion of the slope. This predicted zone of failure matches the location of the head scarps observed in the field. However, not all of the head scarps were at the

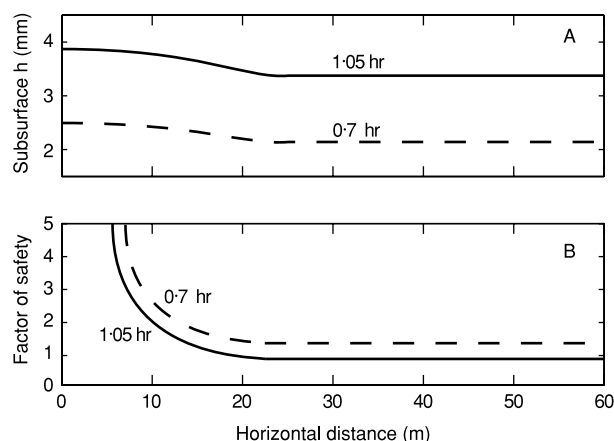


Figure 5. Model results at different times during the simulation. (A) Subsurface flow heights above the hydrophobic layer during the simulation reflect the slope-dependent rainfall intensity. (B) Factor-of-safety values during the simulation. Although flow heights are greater near the divide, the factor of safety is well above unity because of the gentle slopes. The factor of safety drops below unity simultaneously along the entire length of the straight midslope section (see Figure 3 for the hillslope profile)

topographic transition and this may be due to the spatial distribution of burn intensities which affected the emplacement of the hydrophobic layer, both vertically down the soil column and laterally across the burnt area. Further, on a microtopographically complex surface, shallow subsurface flow paths may exhibit considerable convergence and divergence that will determine the specific failure locations.

The model indicates that TDFs may be triggered by small rainstorms. Allowing for apparent cohesion from the fine roots in the crust, however, would increase the amount of rainfall necessary to trigger the TDFs. Unfortunately, measuring the root cohesion of these fine roots is difficult, if not impossible. Nonetheless, the apparent cohesion is likely very low and the results from the model are consistent with field observations made by Wells (1987) who reported that large storms were not necessary to trigger TDFs. Wells (1987) also performed rainfall simulation experiments on burnt hillsides and found that TDFs could be triggered with less than 2.9 mm of total rainfall. This result agrees quite well with the model presented here, which predicts that TDFs will occur with just over 2.6 mm of rain.

TDFs and hillslope evolution

The hillslope profile shown in Figure 3 has a relatively straight midslope segment, a feature common to many hillslopes in the region. Although straight segments are expected at steeper gradients where landsliding produces threshold slopes (Burbank *et al.*, 1996), straight slopes at gentler gradients should be rounded off by diffusive (i.e. solely slope-dependent) processes except where overland flow is a dominant process. For the hillslope shown in Figure 3, infiltration capacities are sufficiently high to prevent the generation of overland flow (Fierer and Gabet, 2002), there is no evidence for recent landsliding, and there is no topographic convergence on the planar slope that would promote shallow landslides. Additionally, in 1997–98, heavy rainfall triggered 86 shallow landslides in coastal sage scrub hillslopes on the property adjacent to Midland School (Gabet and Dunne, 2002) but none of these failures were on gradients gentler than 0.62. The maximum gradient from the profile in Figure 3B is 0.49, suggesting again that the straight midslope segment in Figure 3 cannot be explained by shallow landsliding. A hypothesis explaining the presence of the straight midslope section may involve TDFs. A straight slope initially created by landsliding at steeper gradients may, perhaps, be maintained by TDFs as it relaxes while the hilltop is lowered by diffusive processes.

CONCLUSION

Fire tends to exacerbate hillslope erosion, particularly by concentrating runoff over or within a thin layer of soil. A fire in coastal sage scrub near Santa Barbara, California, provided the opportunity to study post-fire sediment

transport by shallow slope failures. A hydrophobic layer below the soil surface led to the creation of a shallow perched water table that triggered thin debris flows (TDFs). Although the failure depths were only 1–2 cm, their extensive lateral distribution on some hillslopes resulted in substantial amounts of soil being stripped and deposited on valley floors. I present a numerical model that couples an infinite slope stability analysis with subsurface flow routing to examine the process of TDF initiation. The model results agree well with published field experiments that indicate that large rainstorms are not necessary for initiating TDFs on burnt hillslopes.

ACKNOWLEDGEMENTS

I thank Midland School for access to their property before and after the prescribed burn. My gratitude also goes to Dave Bianchi of the Santa Barbara County Fire Department who let me accompany him as he oversaw the prescribed fire. Steve Reneau, Mike Kirkby, and Tom Dunne are gratefully acknowledged for comments on the manuscript. Supplies and salary were supported by U.C. Water Resources Grant UCAL-W-917, a Sigma Xi grant, and a Mildred Mathias grant.

REFERENCES

- Beven K. 1981. Kinematic subsurface stormflow. *Water Resources Research* **17**(5): 1419–1424.
- Burbank DW. *et al.* 1996. Bedrock incision, rock uplift and threshold hillslopes in the northwestern Himalaya. *Nature* **379**: 505–510.
- Cannon SH, Reneau SL. 2000. Conditions for generation of fire-related debris flows, Capulin Canyon, New Mexico. *Earth Surface Processes and Landforms* **25**(10): 1103–1121.
- Cannon SH, Bigio ER, Mine E. 2001. A process for fire-related debris flow initiation, Cerro Grande fire, New Mexico. *Hydrological Processes* **15**: 3011–3023.
- Cerda A. 1998. Changes in overland flow and infiltration after a rangeland fire in a Mediterranean scrubland. *Hydrological Processes* **12**: 1031–1042.
- DeBano LF. 1981. *Water repellent soils: a state of the art*. USDA Forest Service Research Paper, PSW-46.
- DeBano LF, Rice RM, Conrad CE. 1979. *Soil heating in chaparral fires: effects on soil properties, plant nutrients, erosion, and runoff*. USDA Forest Service Research Paper, PSW-145.
- Dibblee TWJ. 1993. *Geologic map of the Figueroa Mountain Quadrangle*. Dibblee Geological Foundation: Santa Barbara, California.
- Dunne T. 1991. Stochastic aspects of the relations between climate, hydrology and landform evolution. *Transactions, Japanese Geomorphological Union*, **12**(1): 1–24.
- Fetter CW. 1997. *Applied Hydrogeology*. Macmillan College Publishing Company: New York.
- Fierer NG, Gabet EG. 2002. Transport of carbon and nitrogen by surface runoff from hillslopes in the Central Coast region of California. *Journal of Environmental Quality* **31**: 1207–1213.
- Gabet EJ. 2003. Sediment transport by dry ravel. *Journal of Geophysical Research* **108**(B1): 2049. DOI: 10.1029/2001JB001686.
- Gabet EJ, Dunne T. 2002. Landslides on coastal sage-scrub and grassland hillslopes in a severe El Niño winter: The effects of vegetation conversion on sediment delivery. *Geological Society of America Bulletin* **114**(8): 983–990.
- Gabet EJ, Dunne T. In press. A stochastic sediment delivery model for a steep Mediterranean landscape. *Water Resources Research*.
- Keeley JE, Fotheringham CJ, Morais M. 1999. Reexamining fire suppression impacts on brushland fire regimes. *Science* **284**: 1829–1832.
- Krammes JS, DeBano LF. 1965. Soil wettability: a neglected factor in watershed management. *Water Resources Research* **1**(2): 283–286.
- Prosser IP, Williams L. 1998. The effect of wildfire on runoff and erosion in native Eucalyptus forest. *Hydrological Processes* **12**: 251–265.
- Richards LA. 1931. Capillary conduction of liquids through porous mediums. *Physics* **1**: 318–333.
- Selby MJ. 1993. *Hillslope Materials and Processes*. Oxford University Press: Oxford.
- Soto B, Diaz-Fierros F. 1998. Runoff and soil erosion from areas of burnt scrub: comparison of experimental results with those predicted by the WEPP model. *Catena* **31**: 257–270.
- Swanson FJ. 1979. *Fire and Geomorphic Processes*. Fire Regimes and Ecosystems Conference. General Technical Report WO-26. USDA Forest Service: Honolulu.
- Wells WG. 1987. The effects of fire on the generation of debris flows in southern California. *Geological Society of America, Reviews in Engineering Geology* **7**: 105–114.